Radboud Repository

Radboud University Nijmegen

PDF hosted at the Radboud Repository of the Radboud University Nijmegen

The following full text is a preprint version which may differ from the publisher's version.

For additional information about this publication click this link.
http://hdl.handle.net/2066/124445

Please be advised that this information was generated on 2017-08-13 and may be subject to change.

EUROPEAN ORGANISATION FOR NUCLEAR RESEARCH

受入
92-10-8/9
高工研図書室

CERN-PPE/92-144
3 September 1992

Evidence for the Existence of the Strange b-flavoured Meson B_s^0 in Z^0 Decays

The OPAL Collaboration

Abstract

We present evidence for the existence of the strange b-flavoured meson B_s^0 in a data sample of 470 628 hadronic Z^0 decays recorded with the OPAL detector at LEP. A signal of $18.3\pm5.2(\text{stat.})\pm0.9(\text{syst.})$ $D_s^-\ell^+$ pairs (or charge conjugate, ℓ=e or $\ell=\mu$) is found after background subtraction, where the D_s meson is detected in the $\phi\pi$ and $K^{*0}K$ final states. Interpreting this signal as coming from the semileptonic decay $B_s^0 \to D_s^-\ell^+\nu X$ and combining the two decay modes of the D_s, we find $f(\overline{b} \to B_s^0) \cdot B(B_s^0 \to D_s^-\ell^+\nu X) \cdot B(D_s^- \to \phi\pi^-) = (3.9\pm1.1(\text{stat.})\pm0.8(\text{syst.}))\times10^{-4}$, where $f(\overline{b} \to B_s^0)$ is the fraction of $\overline{b}$ quarks that result in a B_s^0 meson in Z^0 decays. This signal for the B_s^0 is supported by our observation of an excess of 147 ± 48 inclusive D_s mesons in the $\phi\pi$ and $K^{*0}K$ modes above the number expected from B^0 and B^+ decays and from the fragmentation of primary c quarks. In addition, a search is made for the exclusive decay $B_s^0 \to J/\psi\phi$. Based on one candidate event the 90% confidence level upper limit is determined to be $f(\overline{b} \to B_s^0) \cdot B(B_s^0 \to J/\psi\phi) < 0.22\%$.

(Submitted to Physics Letters B)

The OPAL Collaboration

P.D. Acton[25], G. Alexander[23], J. Allison[16], P.P. Allport[5], K.J. Anderson[9], S. Arcelli[2], A. Astbury[28], D. Axen[29], G. Azuelos[18,a], G.A. Bahan[16], J.T.M. Baines[16], A.H. Ball[17], J. Banks[16], R.J. Barlow[16], S. Barnett[16], J.R. Batley[5], G. Beaudoin[18], A. Beck[23], J. Becker[10], T. Behnke[27], K.W. Bell[20], G. Bella[23], P. Berlich[10], S. Bethke[11], O. Biebel[3], U. Binder[10], I.J. Bloodworth[1], P. Bock[11], B. Boden[3], H.M. Bosch[11], S. Bougerolle[29], H. Breuker[8], R.M. Brown[20], A. Buijs[8], H.J. Burckhart[8], C. Burgard[27], P. Capiluppi[2], R.K. Carnegie[6], A.A. Carter[13], J.R. Carter[5], C.Y. Chang[17], D.G. Charlton[8], P.E.L. Clarke[25], I. Cohen[23], J.C. Clayton[1], W.J. Collins[5], J.E. Conboy[15], M. Cooper[22], M. Coupland[14], M. Cuffiani[2], S. Dado[22], G.M. Dallavalle[2], S. De Jong[8], L.A. del Pozo[5], H. Deng[17], A. Dieckmann[11], M. Dittmar[4], M.S. Dixit[7], E. do Couto e Silva[12], J.E. Duboscq[8], E. Duchovni[26], G. Duckeck[11], I.P. Duerdoth[16], D.J.P. Dumas[6], P.A. Elcombe[5], P.G. Estabrooks[6], E. Etzion[23], H.G. Evans[9], F. Fabbri[2], M. Fincke-Keeler[28], H.M. Fischer[3], D.G. Fong[17], M. Foucher[17], A. Gaidot[21], O. Ganel[26], J.W. Gary[4], J. Gascon[18], R.F. McGowan[16], N.I. Geddes[20], C. Geich-Gimbel[3], S.W. Gensler[9], F.X. Gentit[21], G. Giacomelli[2], V. Gibson[5], W.R. Gibson[13], J.D. Gillies[20], J. Goldberg[22], M.J. Goodrick[5], W. Gorn[4], C. Grandi[2], F.C. Grant[5], J. Hagemann[27], G.G. Hanson[12], M. Hansroul[8], C.K. Hargrove[7], P.F. Harrison[13], J. Hart[8], P.M. Hattersley[1], M. Hauschild[8], C.M. Hawkes[8], E. Heflin[4], R.J. Hemingway[6], R.D. Heuer[8], J.C. Hill[5], S.J. Hillier[1], T. Hilse[10], D.A. Hinshaw[18], J.D. Hobbs[8], P.R. Hobson[25], D. Hochman[26], R.J. Homer[1], A.K. Honma[28,a], C.P. Howarth[15], R.E. Hughes-Jones[16], R. Humbert[10], P. Igo-Kemenes[11], H. Ihssen[11], D.C. Imrie[25], A.C. Janissen[6], A. Jawahery[17], P.W. Jeffreys[20], H. Jeremie[18], M. Jimack[2], M. Jobes[1], R.W.L. Jones[13], P. Jovanovic[1], C. Jui[4], D. Karlen[6], K. Kawagoe[24], T. Kawamoto[24], R.K. Keeler[28], R.G. Kellogg[17], B.W. Kennedy[15], S. Kluth[5], T. Kobayashi[24], T.P. Kokott[3], S. Komamiya[24], L. Köpke[8], J.F. Kral[8], R. Kowalewski[6], J. von Krogh[11], J. Kroll[9], M. Kuwano[24], P. Kyberd[13], G.D. Lafferty[16], F. Lamarche[18], J.G. Layter[4], P. Le Du[21], P. Leblanc[18], A.M. Lee[17], M.H. Lehto[15], D. Lellouch[26], P. Lennert[11], C. Leroy[18], J. Letts[4], S. Levegrün[3], L. Levinson[26], S.L. Lloyd[13], F.K. Loebinger[16], J.M. Lorah[17], B. Lorazo[18], M.J. Losty[7], X.C. Lou[12], J. Ludwig[10], M. Mannelli[8], S. Marcellini[2], G. Maringer[3], C. Markus[3], A.J. Martin[13], J.P. Martin[18], T. Mashimo[24], P. Mättig[3], U. Maur[3], J. McKenna[28], T.J. McMahon[1], J.R. McNutt[25], F. Meijers[8], D. Menszner[11], F.S. Merritt[9], H. Mes[7], A. Michelini[8], R.P. Middleton[20], G. Mikenberg[26], J. Mildenberger[6], D.J. Miller[15], R. Mir[12], W. Mohr[10], C. Moisan[18], A. Montanari[2], T. Mori[24], M. Morii[24], T. Mouthuy[12,b], B. Nellen[3], H.H. Nguyen[9], M. Nozaki[24], S.W. O'Neale[8,c], F.G. Oakham[7], F. Odorici[2], H.O. Ogren[12], C.J. Oram[28,a], M.J. Oreglia[9], S. Orito[24], J.P. Pansart[21], B. Panzer-Steindel[8], P. Paschievici[26], G.N. Patrick[20], N. Paz-Jaoshvili[23], P. Pfister[10], J.E. Pilcher[9], D. Pitman[28], D.E. Plane[8], P. Poffenberger[28], B. Poli[2], A. Pouladdej[6], E. Prebys[8], T.W. Pritchard[13], H. Przysiezniak[18], G. Quast[27], M.W. Redmond[9], D.L. Rees[1], G.E. Richards[16], D. Robinson[8], A. Rollnik[3], J.M. Roney[9], E. Ros[8], S. Rossberg[10], A.M. Rossi[2,d], M. Rosvick[28], P. Routenburg[6], K. Runge[10], O. Runolfsson[8], D.R. Rust[12], M. Sasaki[24], C. Sbarra[8], A.D. Schaile[10], O. Schaile[10], W. Schappert[6], P. Scharff-Hansen[8], P. Schenk[28], H. von der Schmitt[11], S. Schreiber[3], C. Schwick[27], J. Schwiening[3], W.G. Scott[20], M. Settles[12], T.G. Shears[5], B.C. Shen[4], C.H. Shepherd-Themistocleous[7], P. Sherwood[15], R. Shypit[29], A. Simon[3], P. Singh[13], G.P. Siroli[2], A. Skuja[17], A.M. Smith[8], T.J. Smith[8], G.A. Snow[17], R. Sobie[28,e], R.W. Springer[17], M. Sproston[20], K. Stephens[16], J. Steuerer[28], R. Ströhmer[11], D. Strom[30], T. Takeshita[24,f], P. Taras[18], S. Tarem[26], M. Tecchio[9], P. Teixeira-Dias[11], N. Tesch[3], N.J. Thackray[1],

G. Transtromer[25], N.J. Tresilian[16], T. Tsukamoto[24], M.F. Turner[5], G. Tysarczyk-Niemeyer[11], D. Van den plas[18], R. Van Kooten[8], G.J. VanDalen[4], G. Vasseur[21], C.J. Virtue[7], A. Wagner[27], D.L. Wagner[9], C. Wahl[10], J.P. Walker[1], C.P. Ward[5], D.R. Ward[5], P.M. Watkins[1], A.T. Watson[1], N.K. Watson[8], M. Weber[11], P. Weber[6], S. Weisz[8], P.S. Wells[8], N. Wermes[11], M.A. Whalley[1], G.W. Wilson[4], J.A. Wilson[1], V-H. Winterer[10], T. Wlodek[26], S. Wotton[11], T.R. Wyatt[16], R. Yaari[26], A. Yeaman[13], G. Yekutieli[26], M. Yurko[18], W. Zeuner[8], G.T. Zorn[17].

[1]School of Physics and Space Research, University of Birmingham, Birmingham, B15 2TT, UK
[2]Dipartimento di Fisica dell' Università di Bologna and INFN, Bologna, 40126, Italy
[3]Physikalisches Institut, Universität Bonn, D-5300 Bonn 1, FRG
[4]Department of Physics, University of California, Riverside, CA 92521 USA
[5]Cavendish Laboratory, Cambridge, CB3 0HE, UK
[6]Carleton University, Dept of Physics, Colonel By Drive, Ottawa, Ontario K1S 5B6, Canada
[7]Centre for Research in Particle Physics, Carleton University, Ottawa, Ontario K1S 5B6, Canada
[8]CERN, European Organisation for Particle Physics, 1211 Geneva 23, Switzerland
[9]Enrico Fermi Institute and Department of Physics, University of Chicago, Chicago Illinois 60637, USA
[10]Fakultät für Physik, Albert Ludwigs Universität, D-7800 Freiburg, FRG
[11]Physikalisches Institut, Universität Heidelberg, Heidelberg, FRG
[12]Indiana University, Dept of Physics, Swain Hall West 117, Bloomington, Indiana 47405, USA
[13]Queen Mary and Westfield College, University of London, London, E1 4NS, UK
[14]Birkbeck College, London, WC1E 7HV, UK
[15]University College London, London, WC1E 6BT, UK
[16]Department of Physics, Schuster Laboratory, The University, Manchester, M13 9PL, UK
[17]Department of Physics and Astronomy, University of Maryland, College Park, Maryland 20742, USA
[18]Laboratoire de Physique Nucléaire, Université de Montréal, Montréal, Quebec, H3C 3J7, Canada
[20]Rutherford Appleton Laboratory, Chilton, Didcot, Oxfordshire, OX11 0QX, UK
[21]DPhPE, CEN Saclay, F-91191 Gif-sur-Yvette, France
[22]Department of Physics, Technion-Israel Institute of Technology, Haifa 32000, Israel
[23]Department of Physics and Astronomy, Tel Aviv University, Tel Aviv 69978, Israel
[24]International Centre for Elementary Particle Physics and Dept of Physics, University of Tokyo, Tokyo 113, and Kobe University, Kobe 657, Japan
[25]Brunel University, Uxbridge, Middlesex, UB8 3PH UK
[26]Nuclear Physics Department, Weizmann Institute of Science, Rehovot, 76100, Israel
[27]Universität Hamburg/DESY, II Inst für Experimental Physik, 2000 Hamburg 52, Germany
[28]University of Victoria, Dept of Physics, P O Box 3055, Victoria BC V8W 3P6, Canada
[29]University of British Columbia, Dept of Physics, 6224 Agriculture Road, Vancouver BC V6T 1Z1, Canada
[30]University of Oregon, Dept of Physics, Eugene, Oregon 97403, USA

[a]Also at TRIUMF, Vancouver, Canada V6T 2A3
[b]Now at Centre de Physique des Particules de Marseille, Faculté des Sciences de Luminy, Marseille

[c]On leave from Birmingham University, Birmingham B15 2TT, UK
[d]Now at Dipartimento di Fisica, Università della Calabria and INFN, 87036 Rende, Italy
[e]And IPP, McGill University, High Energy Physics Department, 3600 University Str, Montreal, Quebec H3A 2T8, Canada
[f]Also at Shinshu University, Matsumoto 390, Japan

1 Introduction

Decays of the Z^0 boson provide a copious source of b hadrons. Signals for b baryons have been reported by LEP experiments [1]. The existence of the B_s^0 meson[1] (quark composition $\overline{b}s$) is indicated by the large mixing effect observed in the neutral B meson system at high energy e^+e^- and hadron colliders [2]; signals ascribed to semileptonic decays of the B_s^0 have recently been reported [3]. The identification of the B_s^0 meson will allow the measurements of the B_s^0 lifetime and of $B_s^0\overline{B_s^0}$ mixing, which provides information on the Cabibbo-Kobayashi-Maskawa matrix element $|V_{ts}|$ [4].

We consider three different methods for establishing the existence of the B_s^0 meson. The first method is via the decay $B_s^0 \to D_s^- \ell^+ \nu X$ (ℓ = e or $\ell = \mu$). In the spectator model description of B_s^0 decays, this process is expected to dominate the semileptonic decays of the B_s^0, for which the branching ratio is $\sim$11% [5]. The lepton produced in semileptonic b hadron decays is characterised by a large momentum and a large momentum component transverse to the direction of the b hadron. The requirement of such a lepton in an event highly suppresses Z^0 decays into light flavours. Thus the B_s^0 can be effectively tagged through its decay $B_s^0 \to D_s^- \ell^+ \nu X$. Furthermore, the semileptonic decay $B_s^0 \to D_s^- \ell^+ \nu X$ results in a distinct correlation between the electric charge of the D_s meson and that of the charged lepton: only $D_s^- \ell^+$ is formed, whereas $D_s^- \ell^-$ is forbidden, when the lepton stems from a direct decay of the b quark. Background contributions from other processes can be estimated.

The second method is based on an investigation of the inclusive production of D_s mesons in Z^0 decays. The branching ratio for the inclusive decay $B_s^0 \to D_s^- X$ is expected to be large [6]. If the B_s^0 is produced at the expected rate [7], an excess of inclusive D_s production above the contribution from B^+, B^0 decays and charm quark fragmentation should be visible in hadronic decays of the Z^0.

Finally, we consider the exclusive B_s^0 decay into the $J/\psi\phi$ final state. The decay $B_s^0 \to J/\psi\phi$ provides a clean channel in which to search for the B_s^0 directly, although the branching ratio is expected to be rather small [8].

In this paper, we report on an observation of an excess in the yield of $D_s^- \ell^+$ pairs above the expected background. This excess is interpreted as evidence for semileptonic decays of the B_s^0 meson. As corroborating evidence for the B_s^0 we also report an excess of inclusive D_s production above the expectation from B^+, B^0 and primary c quarks. In addition, we describe a search for the exclusive channel $B_s^0 \to J/\psi\phi$.

2 The OPAL detector and hadronic event selection

The OPAL detector has been described in detail in a previous publication [9]. The detector components relevant to the current analyses are described briefly below.

Tracking of charged particles is performed by the central detector consisting of a jet chamber,

[1] Both charge conjugate states are implied throughout this paper.

a vertex detector and chambers measuring the z coordinate[2] of tracks as they leave the barrel region of the jet chamber. The central detector is positioned inside a solenoidal coil, which provides a uniform magnetic field of 0.435 T. The momentum resolution obtained in the barrel region is $\sigma_{p_t}/p_t = \sqrt{(0.02)^2 + (0.0015 \cdot p_t)^2}$, where p_t is the momentum of the charged tracks in the plane perpendicular to the beam axis. In addition to tracking charged particles, the jet chamber provides up to 159 charge samples, resulting in a measurement of the ionisation energy loss of charged particles, which may be used for particle identification. The z coordinates of tracks may be determined from charge division measurements on the jet chamber sense wires, from the vertex detector wires inclined at stereo angles, from hits in the z measuring chambers and, for tracks that pass through the ends of the jet chamber, from the position of the last jet chamber wire hit. One of the latter two measurements is available for approximately 90% of the tracks, resulting in a polar angle resolution of 0.25–2.7 mrad [10]. The coil is surrounded by a time-of-flight counter array and a lead-glass electromagnetic calorimeter with a presampler. Outside the electromagnetic calorimeter is the instrumented return yoke of the magnet, forming the hadron calorimeter, beyond which are muon chambers.

This analysis is based on data recorded with the OPAL detector during the 1990 and 1991 LEP running periods. The data were collected in e^+e^- annihilation at centre-of-mass energies between 88.3 and 94.3 GeV. The selection criteria of hadronic Z^0 decay events have been described in detail elsewhere [11]. The efficiency of the hadronic event selection criteria is determined to be (98.4±0.4)%. After data quality and detector performance requirements, 470 628 events remain in the data sample.

3 Particle identification

The identification of hadron species in this paper relies on ionisation energy loss ($\mathrm{d}E/\mathrm{d}x$) measurements in the jet chamber [12] in the region $|\cos\theta| < 0.94$. A π-K separation of at least 2 standard deviations is obtained, for example, for particles with momenta between 2 and 20 GeV/c in the region $|\cos\theta| < 0.7$. Only particles with more than 20 $\mathrm{d}E/\mathrm{d}x$ samples are identified and used in this analysis. Two levels of identification are used which are defined as follows. We consider a particle as being *consistent* with a specific particle type if its $\mathrm{d}E/\mathrm{d}x$ value is within 3 standard deviations of the expected $\mathrm{d}E/\mathrm{d}x$ for that particle hypothesis with the given momentum. For part of the analysis, *positive identification* of a kaon, with rejection of pions, is used. Positive identification requires that a particle have a $\mathrm{d}E/\mathrm{d}x$ value within 2 standard deviations of the expected $\mathrm{d}E/\mathrm{d}x$ value for a kaon, and more than 1 standard deviation below the $\mathrm{d}E/\mathrm{d}x$ expected for a pion. Positive identification is used only for particles with momenta greater than 2 GeV/c, hence avoiding the regions where $\mathrm{d}E/\mathrm{d}x$ values for various particle species overlap. The positive identification criteria reject more than 84% of the pions according to a Monte Carlo simulation (see section 5.1), and are applied whenever ambiguities between a kaon and a pion can confuse the background with the signal. The efficiency for particle identification is about 95% for the consistency criterion, and ranges from 74% to 84% for the positive identification of charged kaons in the kinematic range relevant to this analysis,

[2] A right-handed coordinate system is adopted by OPAL, where the x axis points to the centre of the LEP ring, and positive z is along the electron beam direction. The angles θ and ϕ are the polar and azimuthal angles, respectively.

as described in sections 4 and 5.

The electron identification procedure used in this paper is the same as that described in a previous publication [13], and more details are given in ref. [14]. Only electrons in the angular range $|\cos\theta| < 0.7$ are identified. The electron identification procedure uses $\mathrm{d}E/\mathrm{d}x$ measured in the jet chamber, shower shape information from the electromagnetic calorimeter and presampler, and E/p, where E is the energy deposited in the calorimeter around the extrapolated position of the central detector track of momentum p. Furthermore, electron candidates which are identified as arising from photon conversions are rejected. In the kinematic range relevant to this analysis (see section 5), the electron identification efficiency is approximately 55%; the probability of misidentifying a hadron as an electron ranges from 0.003% at $p \approx 3$ GeV/c to 0.1% at $p > 10$ GeV/c.

Muons are identified by associating central detector tracks with track segments in the muon detectors, requiring a position match in two orthogonal coordinates. The average identification efficiency is approximately 76% for muons with $p > 3$ GeV/c in the range $|\cos\theta| < 0.9$, as used in this analysis. Hadrons may fake prompt muons either by punch-through or sail-through or by decaying in flight to muons. The average probability for a hadron to fake a prompt muon is estimated to be 0.8% in the kinematic range used in this analysis (see section 5).

4 Reconstruction of the $\mathrm{D_s}$ meson

The strange charmed meson $\mathrm{D_s}$ is reconstructed via the decays $\mathrm{D_s^-} \to \phi\pi^-$ and $\mathrm{D_s^-} \to \mathrm{K^{*0}K^-}$, with branching ratios of (2.8±0.5)% and (2.6±0.5)%, respectively [15]. The ϕ is detected in the $\mathrm{K^+K^-}$ mode, and the $\mathrm{K^{*0}}$ in the $\mathrm{K^+}\pi^-$ mode.

Each event is divided into jets. Tracks used in jet finding are required to fulfil certain quality criteria: a measured distance of closest approach to the nominal $\mathrm{e^+e^-}$ interaction point of less than 5 cm in the x-y plane and 50 cm in the z direction, at least 20 associated jet chamber hits and a minimum momentum of 0.15 GeV/c transverse to the beam axis. Tracks satisfying these criteria and energy clusters [11] in the electromagnetic calorimeter that are not associated with charged tracks are used in the jet finding procedure. We use the scaled mass jet finding algorithm of JADE [16], with the EØ recombination scheme [17] and a value of 0.04 for the jet resolution parameter y_{cut}.

Two different selection criteria are used to select $\mathrm{D_s}$ candidates. We first describe *selection I*, which is used in the inclusive $\mathrm{D_s}$ study to obtain optimal mass resolution of the $\mathrm{D_s}$ signal and to suppress the background. Tracks used to reconstruct the $\mathrm{D_s}$ are required to have a minimum transverse momentum of 0.3 GeV/c and at least 40 associated jet chamber hits, effectively restricting the angular acceptance to $|\cos\theta| < 0.94$. The tracks are further required to have z chamber measurements or z information obtained from the position of the last hit in the jet chamber.

To define ϕ candidates, the invariant mass of pairs of oppositely charged tracks is calculated assuming the kaon mass for each track. Both tracks are required to be positively identified as kaons. For illustration purposes, the resulting $\mathrm{K^+K^-}$ invariant mass distribution is shown in

fig. 1a for K^+K^- pairs with total momenta greater than 6 GeV/c, where a ϕ signal is clearly observed. A K^+K^- pair is considered to be a ϕ candidate if its invariant mass is between 1.005 and 1.035 GeV/c^2. To define K^{*0} candidates, the invariant mass of pairs of oppositely charged tracks is calculated, where the K^+ and π^- are required to be consistent with their assumed particle types and are assigned charged kaon and pion masses, respectively. Also for illustration purposes, the invariant mass distribution for $K^+\pi^-$ pairs with total momenta greater than 6 GeV/c is shown in fig. 1b, where a K^{*0} peak is visible above a large background. A $K^+\pi^-$ pair is considered to be a K^{*0} candidate if its invariant mass is between 0.845 and 0.945 GeV/c^2.

The ϕ candidates are combined with each track which is consistent with being a pion, and the K^{*0} candidates are combined with each track which is positively identified as a kaon. Positive identification is required in the latter case since Monte Carlo simulations show that the decay $D^- \to K^{*0}\pi^-$ will produce an enhancement around the D_s mass if the π^- is misinterpreted as a K^-. In both studies the K^+, K^- and π^- are required to belong to the same jet and to form a vertex in the x-y plane. The vertex requirement is estimated from the data to reject 20% of random combinatorial background, with 97% efficiency for the D_s according to Monte Carlo simulations.

The differences between the angular distributions of D_s decays and those of random combinations are used to suppress the combinatorial background. The D_s is a spin 0 meson, and the final states of both decay modes consist of a spin 1 (ϕ or K^{*0}) vector meson and a spin 0 (π^- or K^-) pseudoscalar meson. The D_s signal is expected to have no dependence on $\cos\theta_p$, where θ_p is the angle between the pseudoscalar meson direction in the rest frame of the D_s and the D_s direction. The $\cos\theta_p$ distribution of the $K^+K^-\pi^-$ combinations in the data, most of which are random combinations, peaks at forward and backward directions. In addition, the $\cos\theta_v$ distribution for D_s decays is proportional to $\cos^2\theta_v$, where θ_v is the angle between the final state pseudoscalar meson from the decay of the vector meson and the D_s in the rest frame of the vector meson. On the other hand, the $\cos\theta_v$ distribution of the random $K^+K^-\pi^-$ combinations in the data is approximately flat. We therefore require $\cos\theta_p < 0.8$ and $|\cos\theta_v| > 0.4$ for the $\phi\pi$ mode. Similarly, we require $|\cos\theta_p| < 0.65$ and $|\cos\theta_v| > 0.6$ for the $K^{*0}K$ mode. The tighter selection criteria are introduced for the $K^{*0}K$ mode to reduce the combinatorial background under the broad K^{*0} resonance, and also because of the difference between the angular distributions of the two D_s decay modes. These requirements reject over 75% (85%) of the random combinatorial background in the $\phi\pi^-$ ($K^{*0}K^-$) mode, as estimated from the data. The efficiency of these requirements from Monte Carlo simulations is determined to be 84% (51%) in the $\phi\pi^-$ ($K^{*0}K^-$) mode.

The invariant mass for $K^+K^-\pi^-$ combinations passing the above requirements is calculated. We show in figs. 2a and 2b the invariant mass distributions of $\phi\pi^-$ and $K^{*0}K^-$ combinations with $x_{KK\pi} > 0.2$, respectively, where $x_{KK\pi} = p_{KK\pi}/E_{\rm beam}$, $p_{KK\pi}$ is the momentum of the $K^+K^-\pi^-$ system and $E_{\rm beam}$ is the beam energy. Enhancements around the D_s mass are observed in both distributions. The fits to the data of figs. 2a and 2b are described in section 6.

For the D_s lepton correlation study, where the combinatorial background is lower due to the high transverse momentum lepton in the event, we define *selection II*, which is optimised for high efficiency. Here we also accept tracks for which the z coordinates are determined only from charge division on the jet chamber wires and/or measurements in the vertex chamber using the stereo wires. In the $\phi\pi^-$ mode the tracks forming the ϕ are required to be consistent

with being kaons. For the $K^{*0}K^-$ mode the same identification criteria as in *selection I* are required. Furthermore, the reconstructed $K^+K^-\pi^-$ vertex is required to lie, in the x-y plane, on the same side of the beam axis as the momentum vector of the $K^+K^-\pi^-$ system. This last criterion rejects 40% of random $KK\pi$ combinations with an estimated efficiency of 89% for the decay $D_s^- \to K^{*0}K^-$.

5 Study of D_s lepton correlations

5.1 The D_s lepton event selection

The B_s^0 is tagged through its semileptonic decay $B_s^0 \to D_s^- \ell^+ \nu X$. The $K^+K^-\pi^-$ combinations selected by *selection II* (see section 4) are analysed together with lepton candidates. The transverse momentum of each lepton candidate, p_T, is calculated with respect to the axis of the jet, where the lepton candidate track is included in the calculation of the jet axis.

In addition to semileptonic decays $B_s^0 \to D_s^- \ell^+ \nu X$ there are other processes producing $D_s^- \ell^+$ events. We have considered the following possible sources of background:

(1) Cascade decays of B^0, B^+ mesons: $\overline{B} \to D_s^- DX$, $D \to \ell^+ X$, as depicted in fig. 3a, where D is a nonstrange charmed meson.

(2) The decays of B^0, B^+ mesons: $B \to D_s^- K \ell^+ \nu X$, as illustrated in fig. 3b, where K is any kaon.

(3) The decays $B \to D^- \ell^+ \nu X$, $D^- \to K^{*0}\pi^-$, part of which may fake a $D_s^- \ell^+$ pair when the pion is misidentified as a kaon.

(4) Random association of D_s^- mesons with genuine leptons other than the background contributions listed above.

(5) Random association of D_s^- mesons with hadrons misidentified as leptons.

We use a Monte Carlo simulation to estimate the reconstruction efficiency for $B_s^0 \to D_s^- \ell^+ \nu X$ and to study these backgrounds. The JETSET 7.2 parton shower Monte Carlo generator [18], with full detector simulation [19], is used to simulate the decay $Z^0 \to b\overline{b}$ as observed in OPAL. The fragmentation is performed using the symmetric LUND fragmentation function with parameters tuned to describe the inclusive distributions of hadronic Z^0 decays [20]. The B_s^0 mass used in the Monte Carlo simulation is 5.48 GeV/c^2, which is consistent with theoretical calculations [21].

The leptons and the D_s^- candidates are required to satisfy:

- $p > 3$ GeV/c and $p_T > 1.2$ GeV/c for the identified leptons,
- $x_{KK\pi} > 0.2$,

- $\cos\theta_{c\ell} > 0.6$, and $3.2 < M(\mathrm{K^+K^-\pi^-\ell}) < 5.5$ GeV/c^2,

where $\theta_{c\ell}$ is the opening angle between the lepton and the $\mathrm{D_s^-}$ candidate, and $M(\mathrm{K^+K^-\pi^-\ell})$ is the invariant mass of the $\mathrm{K^+K^-\pi^-\ell}$ system. The cut $x_{\mathrm{KK}\pi} > 0.2$ removes 74% of random combinatorial background, as estimated from data, with 80% efficiency for the signal. The Monte Carlo simulation indicates that the $\cos\theta_{c\ell}$ cut is 99% efficient for $\mathrm{B_s^0 \to D_s^-\ell^+\nu X}$ decays and rejects 99% of $\mathrm{D_s^-}$ lepton combinations where the $\mathrm{D_s^-}$ and lepton have resulted from the decays of different b hadrons in the same event. In fig. 4, the simulated lepton p_{T} distributions are shown for the signal and for backgrounds (1) and (2). The cut $p_{\mathrm{T}} > 1.2$ GeV/c suppresses these two backgrounds while retaining 60% of the semileptonic $\mathrm{B_s^0}$ decays. After the p_{T} requirement has been applied, the mass cut rejects 24% of random background combinations with only 3% loss in efficiency for $\mathrm{B_s^0 \to D_s^-\ell^+\nu X}$ events.

The $\mathrm{K^+K^-\pi^-}$ invariant mass distributions are shown in figs. 5a and 5b for $\phi\pi^-\ell^+$, $\mathrm{K^{*0}K^-\ell^+}$ and $\phi\pi^-\ell^-$, $\mathrm{K^{*0}K^-\ell^-}$, respectively. An enhancement at the $\mathrm{D_s^-}$ mass is observed in the $\phi\pi^-\ell^+$, $\mathrm{K^{*0}K^-\ell^+}$ combinations, but not in the $\phi\pi^-\ell^-$, $\mathrm{K^{*0}K^-\ell^-}$ combinations. A maximum likelihood fit is performed to these mass distributions. The fit includes a Gaussian signal function with fixed width of 22 MeV/c^2, as obtained by averaging the widths of the $\mathrm{D_s}$ signals observed using *selection II* in the $\phi\pi$ and $\mathrm{K^{*0}K}$ channels. The fit further includes a second order polynomial background distribution, the shape of which is constrained to be the same for both the $(\mathrm{K^+K^-\pi^-})\ell^+$ and $(\mathrm{K^+K^-\pi^-})\ell^-$ combinations. The fit yields 19.2 ± 5.2 $\mathrm{D_s^-\ell^+}$ and 0.4 ± 2.8 $\mathrm{D_s^-\ell^-}$ events, the latter being consistent with no observed signal. A variation of 0.6 $\mathrm{D_s^-\ell^+}$ events is found by changing the width of the Gaussian and the shape of the background distributions used in the fit, which we quote as a systematic error due to the fitting procedure.

5.2 Estimate of backgrounds

The relative importance of backgrounds (1) and (2) has been investigated theoretically [6, 22]. It is expected that the rate for (2) is of the order of a few percent of the total $\mathrm{\overline{B} \to D_s^-X}$ rate. In addition, the decays $\mathrm{\overline{B} \to D_s^-X}$ and $\mathrm{\overline{B} \to D_s^-DX}$ have been studied by experiments performed at the $\Upsilon(4S)$ resonance [23, 24]. The measured $\mathrm{D_s}$ momentum spectrum indicates dominant contributions from two-body and three-body decays involving a $\mathrm{D_s}$ and a nonstrange charmed meson. More directly, the measured branching ratios for $\mathrm{\overline{B} \to D_s^-D}$ account for a large fraction of the inclusive rate for $\mathrm{\overline{B} \to D_s^-X}$ [23, 24]. In our estimation of background contributions, we assume that $\mathrm{\overline{B} \to D_s^-DX}$ (background (1)) accounts for 80% of the inclusive decays $\mathrm{\overline{B} \to D_s^-X}$ and the process shown in fig. 3b (background (2)) accounts for the rest. We use $B(\mathrm{\overline{B} \to D_s^-X})\cdot B(\mathrm{D_s^- \to \phi\pi^-}) = (2.99\pm0.34)\times10^{-3}$, an average of recent measurements from ARGUS and CLEO [23, 24], $B(\mathrm{D_s^- \to K^{*0}K^-})/B(\mathrm{D_s^- \to \phi\pi^-}) = 0.95\pm0.10$ [15], and the Standard Model value of 0.217 for $\Gamma_{\mathrm{b\bar{b}}}/\Gamma_{\mathrm{had}}$ [25], to estimate background contributions from (1) and (2). Monte Carlo simulations predict less than 0.2 events at 90% confidence level (CL) for background (1) and 0.4 ± 0.1 events for background (2) in our data sample.

For background (3), about 32% of the decays $\mathrm{B \to D^-\ell^+\nu X}$, $\mathrm{D^- \to K^{*0}\pi^-}$ will fall within 2 standard deviations of the $\mathrm{D_s}$ mass if the pion is misidentified as a kaon. In the momentum range of this π^-, the misidentification probability with the positive identification criteria for a kaon is about 10%. Assuming $B(\mathrm{B \to D^-\ell^+\nu X}) = 4\%$ [26], $B(\mathrm{D^- \to K^{*0}\pi^-}) = (1.7 \pm 0.8)\%$

[15], and that B^+, B^0 mesons account for 80% of b hadrons produced in Z^0 decays, we estimate that background (3) will contribute 0.3±0.2 events to the $D_s^- \ell^+$ combination in our data.

In addition to decays of B^0 and B^+ mesons, the D_s meson is expected to arise primarily from the following processes: charm hadronisation and decays of excited charmed mesons in $Z^0 \to c\bar{c}$ events and decays of the B_s^0. We have estimated that background (4) contributes less than 0.6 events at 90% CL using Monte Carlo samples of these three processes. We use the data to estimate the contribution from background (5) in the following way. The region in the $K^+K^-\pi^-$ mass distribution between 1.92 and 2.02 GeV/c^2 is defined to be the D_s signal region. The region between 2.04 and 2.14 GeV/c^2 is used as an estimate for combinatorial background under the D_s signal. The numbers of tracks that are not identified as leptons, but pass all other kinematic and acceptance selection criteria for a lepton candidate, as listed in section 5.1, are found to be 276 and 254 in the signal and the sideband regions, respectively. Subtracting the number of tracks in the sideband from the signal region, we find 22±23 tracks associated with the D_s candidates. The known rates for a hadron to be misidentified as a lepton track are used to predict a contribution of 0.2±0.2 $D_s^- \ell^+$ events due to background (5). We also study the Monte Carlo samples used for the evaluation of background (4); no candidate from background (5) is found, resulting in a 90% CL upper limit of 0.6 events on background (5).

Table 1. Estimated background contributions to $D_s^- \ell^+$

Source of Background	Estimated Contribution to $D_s^- \ell^+$
(1) $\overline{B} \to D_s^- DX$, $D \to \ell^+ X$	<0.2 at 90% CL
(2) $B \to D_s^- W^+ KX$, $W^+ \to \ell^+ \nu$	0.4±0.1
(3) $D^- \to K^{*0}\pi^-$, π^- misidentified as K^-	0.3±0.2
(4) Random D_s^--leptons	<0.6 at 90% CL
(5) D_s^- + fake lepton	0.2±0.2
Total	0.9±0.7

The estimated background contributions are summarised in table 1, where the numbers inside the brackets correspond to the listing of sources of background given in section 5.1. Summing the estimated contributions in table 1 and adding the errors and the 90% CL upper limits in quadrature, we expect a total contribution of 0.9±0.7 $D_s^- \ell^+$ events from all the sources of background.

5.3 Results

We subtract background contributions to $D_s^- \ell^+$, as given in table 1, to find 18.3±5.2±0.9 events for $B_s^0 \to D_s^- \ell^+ \nu X$, where the second error is systematic and is obtained by adding in quadrature the uncertainties in the fitting procedure used (±0.6 events) and in our background estimates (±0.7 events).

From Monte Carlo simulations of the analysis, the efficiency[3] for reconstructing $B_s^0 \to D_s^- \ell^+ \nu X$, averaged over the e and μ channels, is found to be (13±1)% for $D_s^- \to \phi\pi^-$ and $\phi \to K^+K^-$, and (8±1)% for $D_s^- \to K^{*0}K^-$ and $K^{*0} \to K^+\pi^-$. The errors are due to the Monte Carlo simulation statistics. Interpreting these events as a signal for B_s^0 and correcting for the branching ratios for $\phi \to K^+K^-$ (0.49±0.01) and $K^{*0} \to K^+\pi^-$ (2/3) [15] and the $D_s^-\ell^+$ reconstruction efficiencies, we measure

$$f(\bar{b} \to B_s^0) \cdot B(B_s^0 \to D_s^- \ell^+ \nu X) \cdot B(D_s^- \to \phi\pi^-) = (3.9 \pm 1.1(\text{stat.}) \pm 0.8(\text{syst.})) \times 10^{-4},$$

where we use the ratio $B(D_s^- \to K^{*0}K^-)/B(D_s^- \to \phi\pi^-)$ to average the results from the two modes, and where $f(\bar{b} \to B_s^0)$ is the B_s^0 production rate per b quark in Z^0 decays. The Standard Model value for $\Gamma_{b\bar{b}}/\Gamma_{had}$ is assumed. The systematic error is due to uncertainties in D_s^- reconstruction efficiency (16%), the lepton identification efficiency (10%), Monte Carlo statistics (6%), uncertainties on $Z^0 \to b\bar{b}$ fragmentation (6%) and the fitting procedure together with the background estimates (5%).

6 Study of inclusive D_s production

In this section the inclusive production of D_s in Z^0 decays is studied and the contributions from known sources are estimated. The mass distributions of the $K^+K^-\pi^-$ selected in section 4 using *selection I* are shown in figs. 2a and 2b for the $\phi\pi$ and $K^{*0}K$ final states, respectively. Fits are performed to the inclusive $K^+K^-\pi^-$ distributions. The background is parametrised with a second order polynomial function, and Gaussian functions are assumed for the D_s and D mass regions. The fit yields the numbers of D_s mesons given in table 2, where the first error is statistical and the second error arises from the choice of different background parametrisations. The fitted mass values for the D_s are 1969±4 MeV/c^2 in the $\phi\pi$ mode and 1969±5 MeV/c^2 in the $K^{*0}K$ mode, in good agreement with the world average mass of the D_s [15]. The fitted widths, 21±3 MeV/c^2 for the $\phi\pi$ mode and 15±5 MeV/c^2 for $K^{*0}K$ mode, are consistent with the expected detector resolution. Combining the two modes, we reconstruct 282±43(stat.)±15(syst.) D_s events.

The contributions to the observed D_s events from c quark fragmentation and from B^0 and B^+ decays are estimated from e^+e^- annihilation data taken at lower energy. The production rate of D_s from B^+ and B^0 decays has been measured by ARGUS and CLEO, as discussed in section 5. The production rate of D_s from $c\bar{c}$ has been determined by the same experiments [24, 27] at a centre-of-mass energy of 10.5 GeV, below the threshold for B meson production. From $\sigma(e^+e^- \to c\bar{c})$ calculated at the same energy [27] and assuming that the D_s production is entirely due to the fragmentation of primary c quarks, one can deduce $f(c \to D_s) \cdot B(D_s^- \to \phi\pi^-) = (0.300 \pm 0.045)\%$. Here $f(c \to D_s)$ denotes the probability that a primary c quark picks up a strange quark from $s\bar{s}$ pairs produced in the colour field to form a D_s, which we assume is independent of the centre-of-mass energy [28].

To determine the detection efficiencies, assumptions are made on the decay rates of B mesons. The Monte Carlo simulation for D_s produced in B^+ and B^0 decays is based on the

[3]Small differences are noticed between the efficiencies for hadron identification, lepton identification and charged particle tracking predicted by the Monte Carlo simulations and those determined from the data; corrections are made to these efficiencies to account for these differences.

Bauer-Stech-Wirbel model [29] for two-body decays of B states. The fraction of two-body decays has been fixed to be the combined ARGUS and CLEO result of (56.9±7.5)% [23, 24]. The remaining decays are assumed to be three-body decays with additional π, ρ and ω in equal proportions. This Monte Carlo model adequately describes the momentum distribution of the D_s produced in B decays at the $\Upsilon(4S)$ [24].

In order to estimate a systematic error on the prediction for B^+ and B^0 decays into final states containing a D_s, we vary the two-body decay fraction in the allowed range and include that predicted by JETSET 7.2. The energy dependence of the fragmentation is parametrised by the Peterson functional form [30] with ϵ_b in the range $0.0017 < \epsilon_b < 0.0053$. We also include the prediction of the LUND symmetric scheme with Bowler modification [31] in estimating the systematic error. The fraction of D_s mesons passing the $x_{KK\pi} > 0.2$ criterion is determined to be 0.78±0.11(syst.).

The fragmentation of c quarks has been studied by OPAL based on muons [32] and D^* mesons [33] produced in hadronic Z^0 decays. In the following discussion, the possible difference in kinematics between the D^* and the primary c hadrons produced in $Z^0 \to c\bar{c}$ events is neglected. Averaging the nearly independent measurements of the mean fractional energy of primary c hadrons, $\langle x_E \rangle$, gives $\langle x_E \rangle = 0.52 \pm 0.02$. The energy dependence of the fragmentation is parametrised by the Peterson functional form with $0.06 < \epsilon_c < 0.08$ for the $\langle x_E \rangle$ range given above. The systematic error due to a variation in the conservative range $0.02 < \epsilon_c < 0.12$ is small; larger variations occur in the case of the LUND symmetric scheme with and without Bowler modification, which we have included in the systematic error. The fraction of D_s mesons passing the $x_{KK\pi} > 0.2$ criterion is determined to be 0.913±0.012(syst.).

The reconstruction efficiencies of *selection I* have been determined from the Monte Carlo simulations for $x_{KK\pi} > 0.2$. The average detection efficiency for the $D_s^- \to \phi\pi^- \to K^+K^-\pi^-$ decay is found to be (16.2±2.0)% and that for $D_s^- \to K^{*0}K^- \to K^+K^-\pi^-$ is (12.9±1.8)%, not including the branching ratios for the ϕ and K^{*0} decays. The errors on the efficiencies include a systematic contribution due to the modelling of the dE/dx (6%) and the mass resolution (10%). Both efficiencies show little dependence on the D_s momentum.

Table 2 gives the estimates for the numbers of D_s from primary c quarks and from B^0, B^+ mesons. We assume the Standard Model values of 0.172 for $\Gamma_{c\bar{c}}/\Gamma_{had}$ and of 0.217 for $\Gamma_{b\bar{b}}/\Gamma_{had}$ [25] and take the probability to form a B^0 or B^+ from a primary b quark to be (80±20)%[4].

Table 2. Contributions to inclusive D_s signal

	Number of events in $\phi\pi$ channel	Number of events in $K^{*0}K$ channel
Data	157±26(stat.)±13(syst.)	125±34(stat.)±8(syst.)
Predicted D_s from $c\bar{c}$	35±7(syst.)	38±8(syst.)
Predicted D_s from B^+, B^0	31±10(syst.)	31±11(syst.)
Excess	91 ± 32	56 ± 38

Subtracting the predicted contributions from the observed numbers of D_s in the $x_{KK\pi} > 0.2$ range, we find an excess of events in each D_s decay mode (see table 2). We add the numbers of

[4]Since we subtract the estimate for the number of D_s from B^0 and B^+, the most conservative estimate includes the possibility that no B_s^0 or b-flavoured baryons are produced from primary b quarks.

D_s in the $\phi\pi$ and $K^{*0}K$ modes from the data and subtract the sum of the predicted numbers of D_s, taking into account the correlated systematic errors. We thus determine the combined excess of D_s to be 147 ± 48 events, corresponding to a 3 standard deviation effect. If we interpret this excess as being entirely due to $B_s^0 \to D_s^- X$ decays, we estimate

$$f(\overline{b} \to B_s^0) \cdot B(B_s^0 \to D_s^- X) \cdot B(D_s^- \to \phi\pi^-) = (5.9 \pm 1.9 \pm 1.1) \times 10^{-3}.$$

Here a weighted average of the results for the $D_s \to \phi\pi$ and $D_s \to K^{*0}K$ channels is calculated, using the measured ratio of the two decay rates. The Standard Model value for $\Gamma_{b\overline{b}}/\Gamma_{had}$ is assumed. The first error is the error on the combined number of excess D_s events obtained above. We have added a second systematic error which is due to the uncertainties in the kinematic acceptance and detection efficiency for $B_s^0 \to D_s^- X$.

As a consistency check we construct the x_{D_s} distributions for the D_s signal. The signal is obtained by performing fits as described above to the $K^+K^-\pi^-$ invariant mass distributions for the $\phi\pi$ and $K^{*0}K$ decay channels in bins of $x_{KK\pi}$. The x_{D_s} distributions for the $\phi\pi$ and $K^{*0}K$ channels are shown in figs. 6a and 6b, respectively. Since the average momentum of D_s mesons from c quark fragmentation is higher than that from b quarks, the x_{D_s} distribution can be used to estimate the fraction of D_s from b hadrons. A fit is performed to the measured x_{D_s} distribution in the range $0.2 < x_{D_s} < 1.0$ using the predicted shapes of the x_{D_s} distribution for $c \to D_s$ and $b \to D_s$. Studies employing the Monte Carlo models described above show that the x_{D_s} distribution from B_s^0 decays differs little from that from B^0 or B^+. Assuming both distributions to be the same, this fit yields an estimate of the $c \to D_s$ contribution without assuming the measured rate in [27]. The fit results in 52 ± 25 $c \to D_s$ events in the $\phi\pi$ channel and 26 ± 15 events in the $K^{*0}K$ channel, consistent with the estimates obtained by using the ARGUS and CLEO measurements (in table 2). However, the error, which includes a systematic component obtained by varying the models for c and b quark fragmentation as discussed above, is larger.

7 Search for the decay $B_s^0 \to J/\psi\phi$

We have also searched directly for the B_s^0 in the decay channel $B_s^0 \to J/\psi\phi$. The branching ratio for this process has been calculated, for example, using the Bauer-Stech-Wirbel model [29] to be 0.13% with a large uncertainty [8].

The selection of J/ψ candidates in the $\mu^+\mu^-$ and e^+e^- decay channels is similar to that described in ref. [34]. The minimum momentum of the lepton candidates is 2 GeV/c. The lepton identification procedure used here is not the same as in the rest of the paper. The two leptons from the J/ψ decay are required to be no more than 60° apart. In the analysis, an oppositely-signed lepton pair is taken to be a J/ψ candidate if the di-lepton invariant mass is in the range $2.95 - 3.30$ GeV/c^2 for $\mu^+\mu^-$ and $2.85 - 3.30$ GeV/c^2 for e^+e^-. The efficiencies for detecting J/ψ mesons in these mass ranges are $(40.5\pm4.5)\%$ and $(23.9\pm3.5)\%$ for $\mu^+\mu^-$ and e^+e^-, respectively. Approximately 120 J/ψ decays are found above an estimated background of 22 events.

The ϕ candidates with a total momentum exceeding 4 GeV/c are selected as in section 4. For highest efficiency, less stringent particle identification criteria are applied here. Tracks that

are associated with less than 20 $\mathrm{d}E/\mathrm{d}x$ measurements remain in the analysis without requiring particle identification. For tracks with at least 20 $\mathrm{d}E/\mathrm{d}x$ measurements the $\mathrm{d}E/\mathrm{d}x$ values are required to be compatible at the 98% CL with the expected value for kaons, if the measured $\mathrm{d}E/\mathrm{d}x$ value is higher than the expected value[5].

The energy of the reconstructed $\mathrm{B_s^0}$ candidates is required to be at least 30% of the beam energy. Once the J/ψ has been detected, the detection efficiency for $\phi \to \mathrm{K^+K^-}$ from the decay $\mathrm{B_s^0} \to$ J/$\psi\phi$ is found from Monte Carlo simulations to be (50.4±3.7)%.

One event is found with a J/$\psi\phi$ invariant mass greater than 5.0 GeV/c^2. The invariant mass value is 5.36 GeV/c^2. The resolution in the invariant mass is estimated by Monte Carlo simulations to be 70 MeV/c^2. The $\mathrm{B_s^0}$ candidate carries 77% of the beam energy.

Using $B(\mathrm{J}/\psi \to \mu^+\mu^-) = (5.97\pm0.25)\%$ [15], assuming the same for the electron channel and using the branching ratio for $\phi \to \mathrm{K^+K^-}$, we determine the combined efficiency for detecting the decay chain $\mathrm{B_s^0} \to$ J/$\psi\phi \to \ell^+\ell^-\mathrm{K^+K^-}$ to be (0.48±0.08)%, averaging over the electron and muon channels. From the one observed $\mathrm{B_s^0}$ candidate, assuming the Standard Model value for $\Gamma_{\mathrm{b\bar{b}}}/\Gamma_{\mathrm{had}}$, we determine the upper limit $f(\overline{\mathrm{b}} \to \mathrm{B_s^0}) \cdot B(\mathrm{B_s^0} \to \mathrm{J}/\psi\phi) < 0.22\%$ at the 90% CL. Assuming $f(\overline{\mathrm{b}} \to \mathrm{B_s^0}) = 12\%$ and $B(\mathrm{B_s^0} \to \mathrm{J}/\psi\phi) = 0.13\%$ [8], we would expect 0.4 reconstructed $\mathrm{B_s^0} \to$ J/$\psi\phi$ decays in our data sample.

8 Summary of results and conclusions

Using 470 628 hadronic $\mathrm{Z^0}$ decays collected with the OPAL detector, evidence is found for the existence of the strange b-flavoured meson $\mathrm{B_s^0}$. A signal of 18.3±5.2(stat.)±0.9(syst.) events ascribed to $\mathrm{B_s^0} \to \mathrm{D_s^-}\ell^+\nu\mathrm{X}$ is observed. Combining the two decay modes of the $\mathrm{D_s}$ and averaging over the e and μ channels, the product branching ratio $f(\overline{\mathrm{b}} \to \mathrm{B_s^0}) \cdot B(\mathrm{B_s^0} \to \mathrm{D_s^-}\ell^+\nu\mathrm{X}) \cdot B(\mathrm{D_s^-} \to \phi\pi^-)$ is measured to be $(3.9\pm1.1(\mathrm{stat.})\pm0.8(\mathrm{syst.}))\times10^{-4}$.

As a consistency check, we estimate $f(\overline{\mathrm{b}} \to \mathrm{B_s^0})$. We use $B(\mathrm{D_s^-} \to \phi\pi^-)$=(2.8±0.5)% [15] and assume $B(\mathrm{B_s^0} \to \mathrm{D_s^-}\ell^+\nu\mathrm{X})$ =11% [15, 35]. The rate $f(\overline{\mathrm{b}} \to \mathrm{B_s^0})$ is estimated to be (12.7±3.6±2.3)%, consistent with the expected rate [7]. The second error is due to the error on the branching ratio $\mathrm{D_s^-} \to \phi\pi^-$. We do not assign a systematic error due to the uncertainty on $B(\mathrm{B_s^0} \to \mathrm{D_s^-}\ell^+\nu\mathrm{X})$.

The signal for $\mathrm{B_s^0} \to \mathrm{D_s^-}\ell^+\nu\mathrm{X}$ is corroborated by an excess of 147 ± 48 inclusive $\mathrm{D_s}$ mesons beyond those expected from $\mathrm{B^0}$ or $\mathrm{B^+}$ decays and from primary c quark fragmentation. If we assume that this excess is entirely due to $\mathrm{B_s^0} \to \mathrm{D_s^-X}$ decays, we can estimate the product branching ratio $f(\overline{\mathrm{b}} \to \mathrm{B_s^0}) \cdot B(\mathrm{B_s^0} \to \mathrm{D_s^-X}) \cdot B(\mathrm{D_s^-} \to \phi\pi^-) = (5.9 \pm 1.9 \pm 1.1) \times 10^{-3}$. This value is a weighted average of the $\phi\pi$ and $\mathrm{K^{*0}K}$ channels, using the measured ratio of the two decay rates. The reconstructed $x_{\mathrm{D_s}}$ distributions are found to be consistent with the excess originating from the decay $\mathrm{B_s^0} \to \mathrm{D_s^-X}$.

[5]Since almost all kaon candidates have momenta exceeding 2 GeV/c, their expected $\mathrm{d}E/\mathrm{d}x$ values are lower than those of pions, which are the dominant background, and higher than those of protons of the same momentum.

A search is made for the exclusive decay $B_s^0 \rightarrow J/\psi\phi$. One candidate event is found. We determine the 90% CL upper limit of $f(\overline{b} \rightarrow B_s^0) \cdot B(B_s^0 \rightarrow J/\psi\phi) < 0.22\%$.

Acknowledgements

It is a pleasure to thank the SL Division for the efficient operation of the LEP accelerator, the precise information on the absolute energy, and their continuing close cooperation with our experimental group. In addition to the support staff at our own institutions we are pleased to acknowledge the Department of Energy, USA, National Science Foundation, USA, Science and Engineering Research Council, UK, Natural Sciences and Engineering Research Council, Canada, Israeli Ministry of Science, Minerva Gesellschaft, Japanese Ministry of Education, Science and Culture (the Monbusho) and a grant under the Monbusho International Science Research Program, American Israeli Bi-national Science Foundation, Direction des Sciences de la Matière du Commissariat à l'Energie Atomique, France, Bundesministerium für Forschung und Technologie, FRG, National Research Council of Canada, Canada, A.P. Sloan Foundation and Junta Nacional de Investigação Científica e Tecnológica, Portugal.

References

[1] ALEPH Collab., D. Decamp *et al.*, Phys. Lett. **B 278** (1992) 209;
OPAL Collab., P. D. Acton *et al.*, Phys. Lett. **B 281** (1992) 394.

[2] The average mixing in the neutral B meson system at the Sp$\overline{\text{p}}$S, the Tevatron and LEP is large, indicating indirectly the production of B_s^0:
ALEPH Collab., D. Decamp *et al.*, Phys. Lett. **B 258** (1991) 236;
CDF Collab., F. Abe *et al.*, Phys. Rev. Lett. **67** (1991) 3351;
L3 Collab., B. Adeva *et al.*, Phys. Lett. **B 252** (1990) 703;
MAC Collab., H. Band *et al.*, Phys. Lett. **B 200** (1988) 221;
MARK II Collab., A. J. Weir *et al.*, Phys. Lett. **B 240** (1990) 703;
OPAL Collab., P. D. Acton *et al.*, Phys. Lett. **B 276** (1992) 379;
UA1 Collab., C. Albajar *et al.*, Phys. Lett. **B 262** (1991) 171.

[3] ALEPH Collab., D. Buskulic *et al.*, CERN-PPE/92-73, submitted to Phys. Lett.;
DELPHI Collab., P. Abreu *et al.*, CERN-PPE/92-104, submitted to Phys. Lett.

[4] See for example: P. J. Franzini, Phys. Rep. **173** (1989) 1.

[5] D. Du and Z. Wang, Phys. Rev. **D 38** (1988) 3570.

[6] M. Suzuki, Phys. Rev. **D 31** (1985) 1158; LBL Preprint LBL-18796.
$B(B_s^0 \to D_s^- X)$ is predicted to be $0.86^{+0.08}_{-0.13}$.

[7] A B_s^0 production rate of $\sim$12% per $\overline{\text{b}}$ quark in Z^0 decays is expected. See:
J. H. Kühn and P. M. Zerwas, in Z physics at LEP1, ed. G. Altarelli *et al.*,
CERN89-08, Vol. 1 (1989) 267.

[8] J. Bijnens and F. Hoogeveen, Phys. Lett. **B 283** (1992) 434.

[9] OPAL Collab., K. Ahmet *et al.*, Nucl. Instrum. and Meth. **A 305** (1991) 275.

[10] O. Biebel *et al.*, CERN-PPE/92-55, submitted to Nucl. Instrum. and Meth.

[11] OPAL Collab., G. Alexander *et al.*, Z. Phys. **C 52** (1991) 175.

[12] M. Hauschild *et al.*, Nucl. Instrum. and Meth. **A 314** (1992) 74.

[13] OPAL Collab., P. D. Acton *et al.*, Phys. Lett. **B 276** (1992) 379.

[14] OPAL Collab., P. D. Acton *et al.*, CERN-PPE/92-38, to be published in Z. Phys. C.

[15] Particle Data Group, K. Hikasa *et al.*, Phys. Rev. **D 45** (1992) I.1.

[16] JADE Collab., S. Bethke *et al.*, Phys. Lett. **B 213** (1988) 235.

[17] OPAL Collab., M. Z. Akrawy *et al.*, Z. Phys. **C 49** (1991) 375.

[18] T. Sjöstrand, Int. J. of Mod. Phys. **A 3** (1988) 751.

[19] J. Allison *et al.*, Nucl. Instrum. and Meth. **A 317** (1992) 47.

[20] OPAL Collab., M. Akrawy *et al.*, Z. Phys. **C 47** (1990) 505.

[21] W. Kwong and J. L. Rosner, Phys. Rev. **D 44** (1991) 212.

[22] A. Ali, Z. Phys. **C 1** (1979) 269;
F. Hussain, M. D. Scadron, Phys. Rev. **D 30** (1984) 1492;
E. Golowich *et al.*, Z. Phys. **C 48** (1990) 89.

[23] CLEO Collab., D. Bortoletto *et al.*, Phys. Rev. Lett. **64** (1990) 2117.

[24] ARGUS Collab., H. Albrecht *et al.*, DESY 91-121.

[25] D. Bardin *et al.*, CERN-TH.6443/92 (1992) (unpublished).

[26] ARGUS Collab., H. Albrecht *et al.*, DESY 92-029.
The branching ratio $B(\mathrm{D}^*(2010)^- \to \mathrm{D}^-\mathrm{X}) = (45.2 \pm 4.7)\%$, as given in ref. 14, is used to estimate $B(\mathrm{B} \to \mathrm{D}^-\ell^+\nu\mathrm{X})$.

[27] CLEO Collab., D. Bortoletto *et al.*, Phys. Rev. **D 37** (1988) 1719.

[28] For the probability to pick up $\mathrm{s\bar{s}}$ pairs from the sea as measured by strange meson and baryon production at LEP, see:
OPAL Collab., M. Z. Akrawy *et al.*, Phys. Lett. **B 264** (1991) 467;
OPAL Collab., P. Acton *et al.*, CERN-PPE/92-118, submitted to Phys. Lett.

[29] M. Bauer, B. Stech and M. Wirbel, Z. Phys. **C 34** (1987) 103.

[30] C. Peterson *et al.*, Phys. Rev. **D 27** (1983) 105.

[31] M. G. Bowler, Z. Phys. **C 11** (1981) 169;
T. Sjöstrand, CERN-TH-6488-92 (1992) 202.

[32] OPAL Collab., M. Z. Akrawy *et al.*, Phys. Lett. **B 263** (1991) 311.

[33] OPAL Collab., G. Alexander *et al.*, Phys. Lett. **B 262** (1991) 341.

[34] OPAL Collab., G. Alexander *et al.*, Phys. Lett. **B 266** (1991) 485.

[35] The average semileptonic branching ratio of B hadrons at LEP is compatible with being 11%. See references below:
ALEPH Collab., D. Decamp *et al.*, Phys. Lett. **B 244** (1990) 551;
DELPHI Collab., P. Abreu *et al.*, CERN-PPE/90-118;
L3 Collab., B Adeva *et al.*, Phys. Lett. **B 261** (1991) 177;
OPAL Collab., M. Z. Akrawy *et al.*, Phys. Lett. **B 263** (1991) 311;
OPAL Collab., P. D. Acton *et al.*, CERN-PPE/92-38, to be published in Z. Phys. **C**.

Figure Captions

Fig. 1.
(a) The invariant mass distribution of candidate K^+K^- pairs with total momenta greater than 6 GeV/c.
(b) The invariant mass distribution of candidate $K^+\pi^-$ pairs with total momenta greater than 6 GeV/c.
The ϕ signal is parametrised with two Gaussian functions of different widths, above a background distribution estimated using a 5th order polynomial function. The $K^+\pi^-$ invariant mass distribution is fitted to a K^{*0} signal form and a background distribution estimated using a 5th order polynomial function. In both case, the dashed line represents the estimated background distribution in the signal region.

Fig. 2.
(a) The $\phi\pi$ invariant mass distribution for $x_{KK\pi} > 0.2$, where the ϕ is reconstructed in the K^+K^- channel. Gaussian distributions are fitted to the D^+ and D_s mass regions.
(b) The $K^{*0}K$ invariant mass distribution for $x_{KK\pi} > 0.2$, where the K^{*0} is reconstructed in the $K^+\pi^-$ channel. Gaussian distributions are fitted to the D^+ and the D_s mass regions.
The dashed lines are the estimated background distributions in the charm signal regions. The solid line distributions include the charm signal contributions in addition to background contributions which are estimated using second order polynomial functions.

Fig. 3. Decay diagrams for:
(a) $\overline{B} \to D_s^- D$, and
(b) $B \to D_s^- \ell^+ \nu K$, where the $\ell^+\nu$ pair originates from the W^+ vertex.

Fig. 4. Lepton p_T distributions for:
(a) $B_s^0 \to D_s^- \ell^+ \nu X$;
(b) $\overline{B} \to D_s^- D$, $D \to \ell^+ \nu X$, and
(c) $B \to D_s^- \ell^+ \nu K$, where the $\ell^+\nu$ pair originates from the W^+ vertex.
These distributions are based on 1000 Monte Carlo events for each case. The cut $x_{KK\pi} > 0.2$ is applied and the leptons are identified.

Fig. 5. Invariant mass distributions of $\phi\pi^-$ and $K^{*0}K^-$ for:
(a) $K^+K^-\pi^-\ell^+$ combinations, and
(b) $K^+K^-\pi^-\ell^-$ combinations.

Fig. 6. Inclusive x_{D_s} distributions, normalised to one, for:
(a) $\phi\pi$, and
(b) $K^{*0}K$.
The solid dots represent the data. The shaded area represents the contributions from $c \to D_s$ and the remaining area below the dashed line represents the contributions from $b \to D_s$, assuming identical momentum distributions for B^0, B^+ and B_s^0.

Figure 1

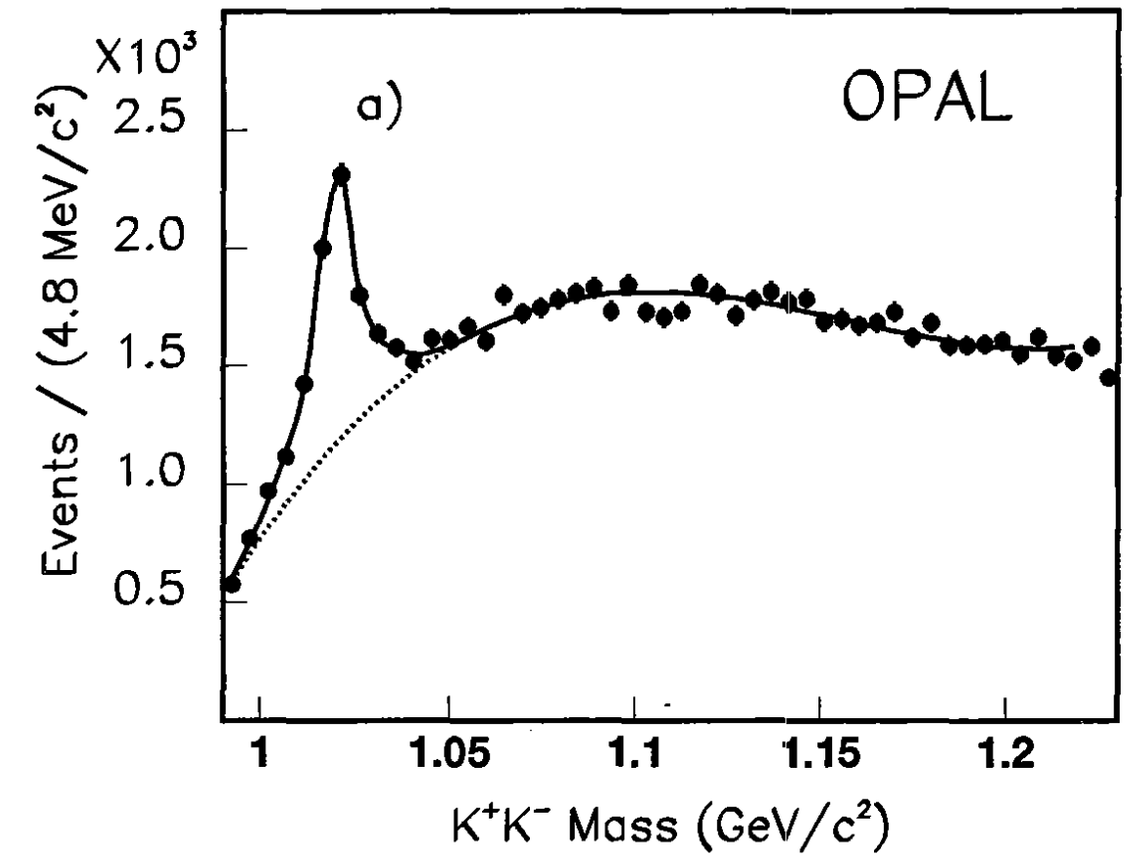
a)
OPAL
X10³
2.5
2.0
1.5
1.0
0.5
Events / (4.8 MeV/c²)
1
1.05
1.1
1.15
1.2
K⁺K⁻ Mass (GeV/c²)

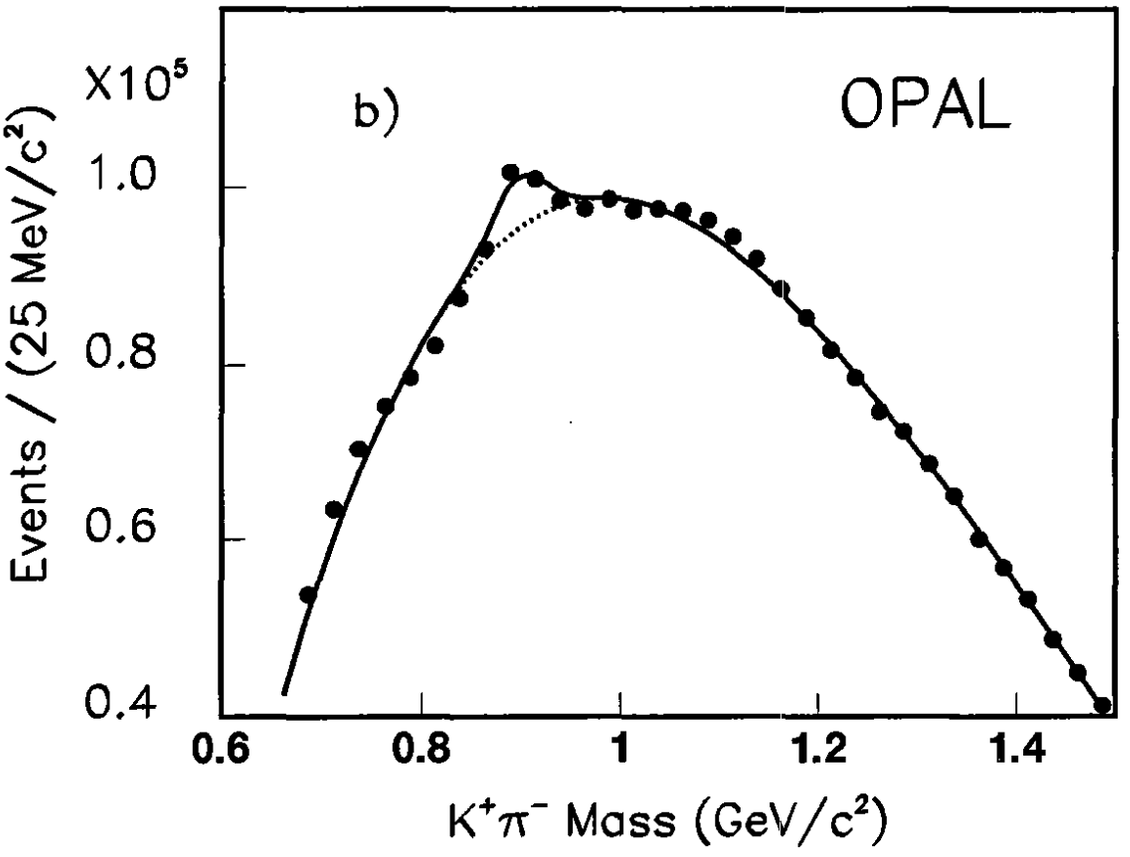
b)
OPAL
X10⁵
1.0
0.8
0.6
0.4
Events / (25 MeV/c²)
0.6
0.8
1
1.2
1.4
K⁺π⁻ Mass (GeV/c²)

Figure 2

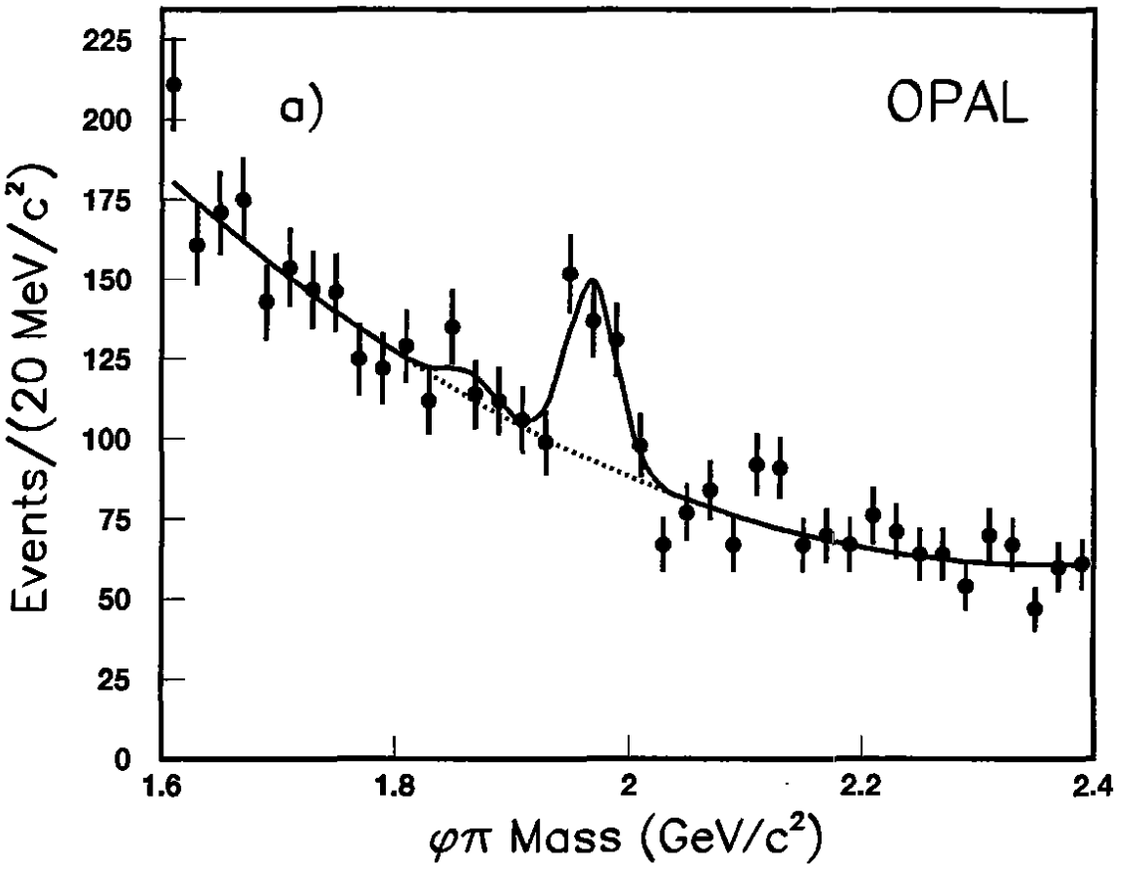
a)
OPAL
Events/(20 MeV/c²)
225
200
175
150
125
100
75
50
25
0
1.6
1.8
2
2.2
2.4
φπ Mass (GeV/c²)

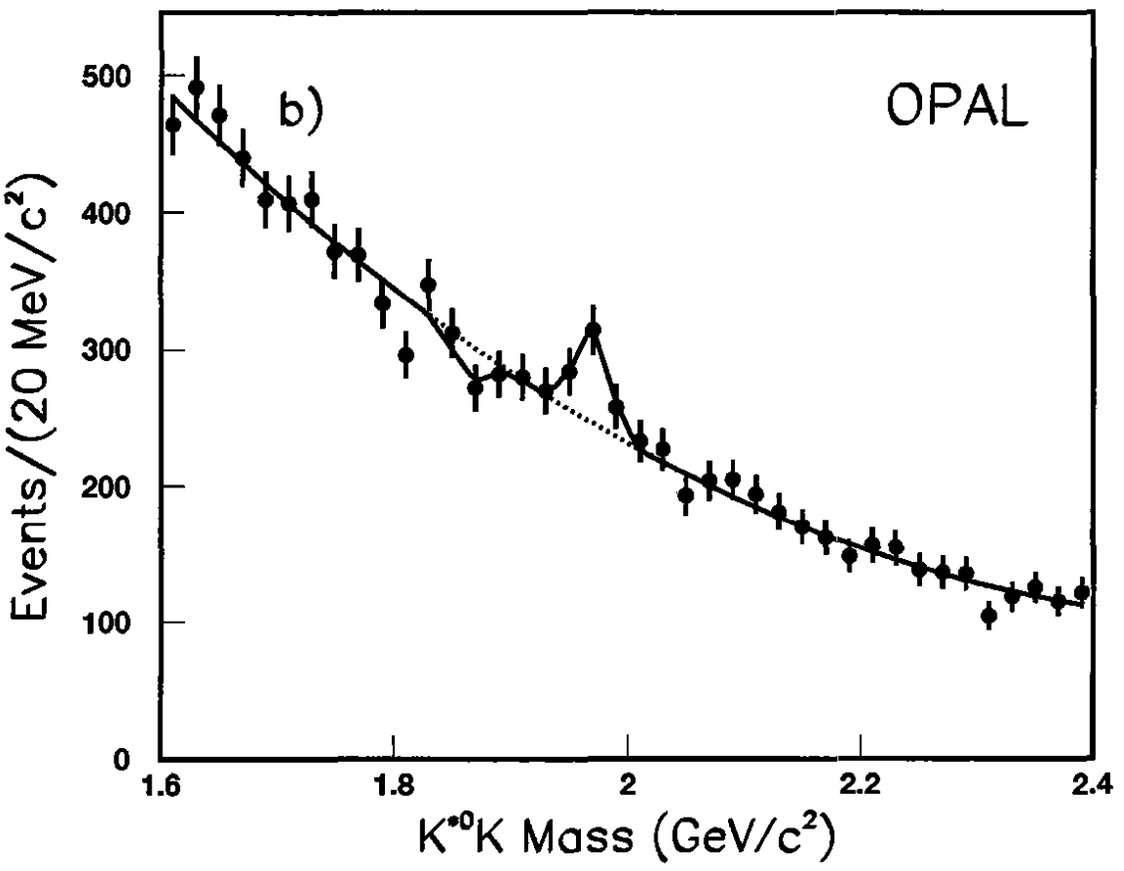
b)
OPAL
Events/(20 MeV/c²)
500
400
300
200
100
0
1.6
1.8
2
2.2
2.4
K*0K Mass (GeV/c²)

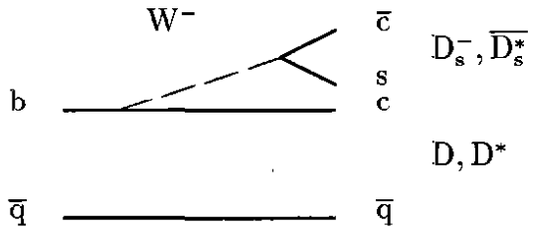

(a) $\overline{B} \to D_s^{-(*)} D^{(*)}$

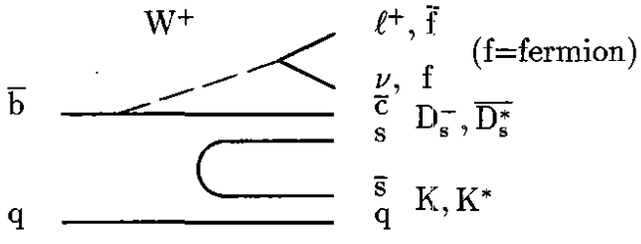

(b) $B \to D_s^{-(*)} \ell^+ \nu K^{(*)}$

Figure 3

Figure 4

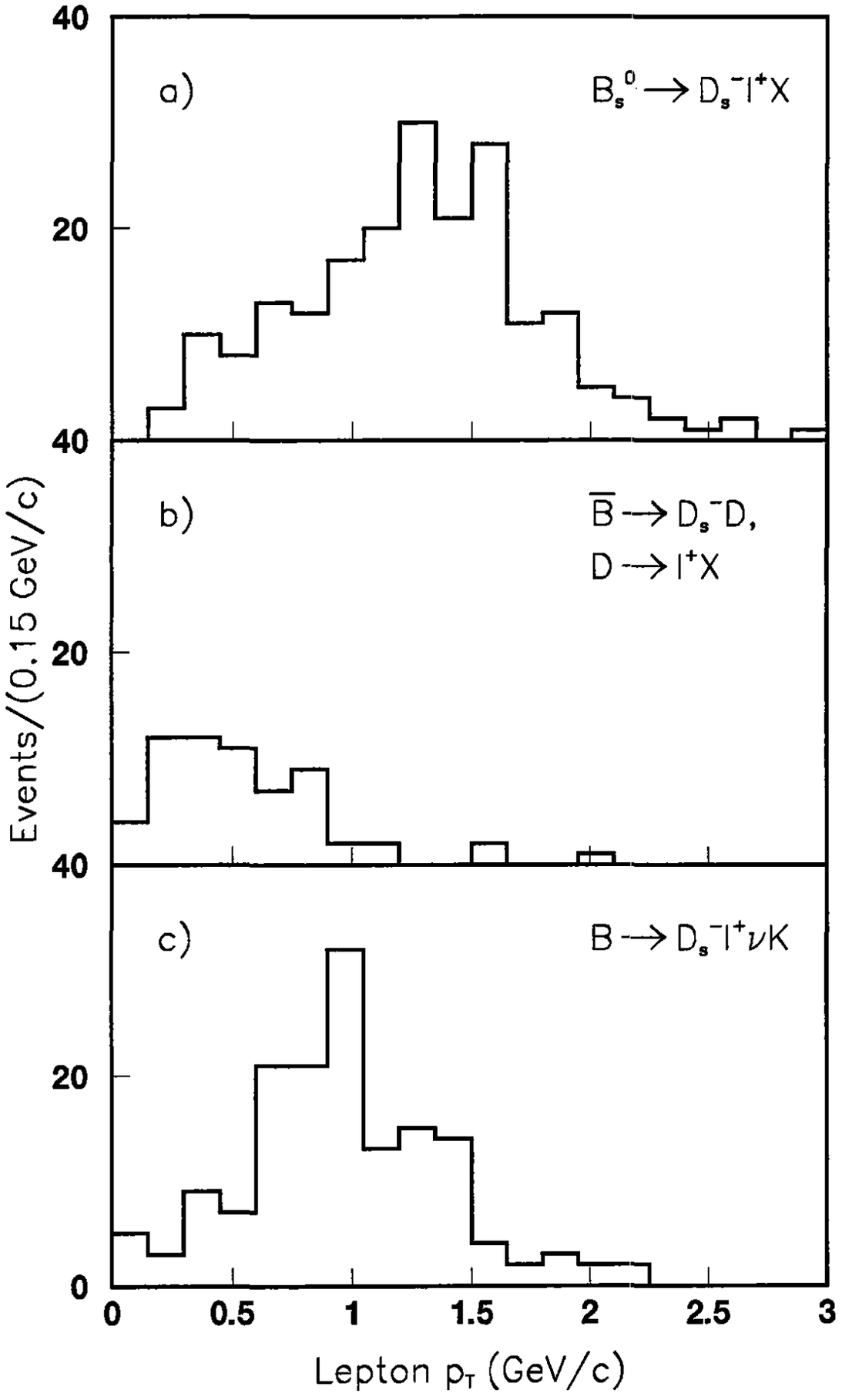
a)
$B_s^0 \rightarrow D_s^- l^+ X$
b)
$\overline{B} \rightarrow D_s^- D$,
$D \rightarrow l^+ X$
c)
$B \rightarrow D_s^- l^+ \nu K$
Events/(0.15 GeV/c)
Lepton p_T (GeV/c)
0
20
40
0.5
1
1.5
2
2.5
3

Figure 5

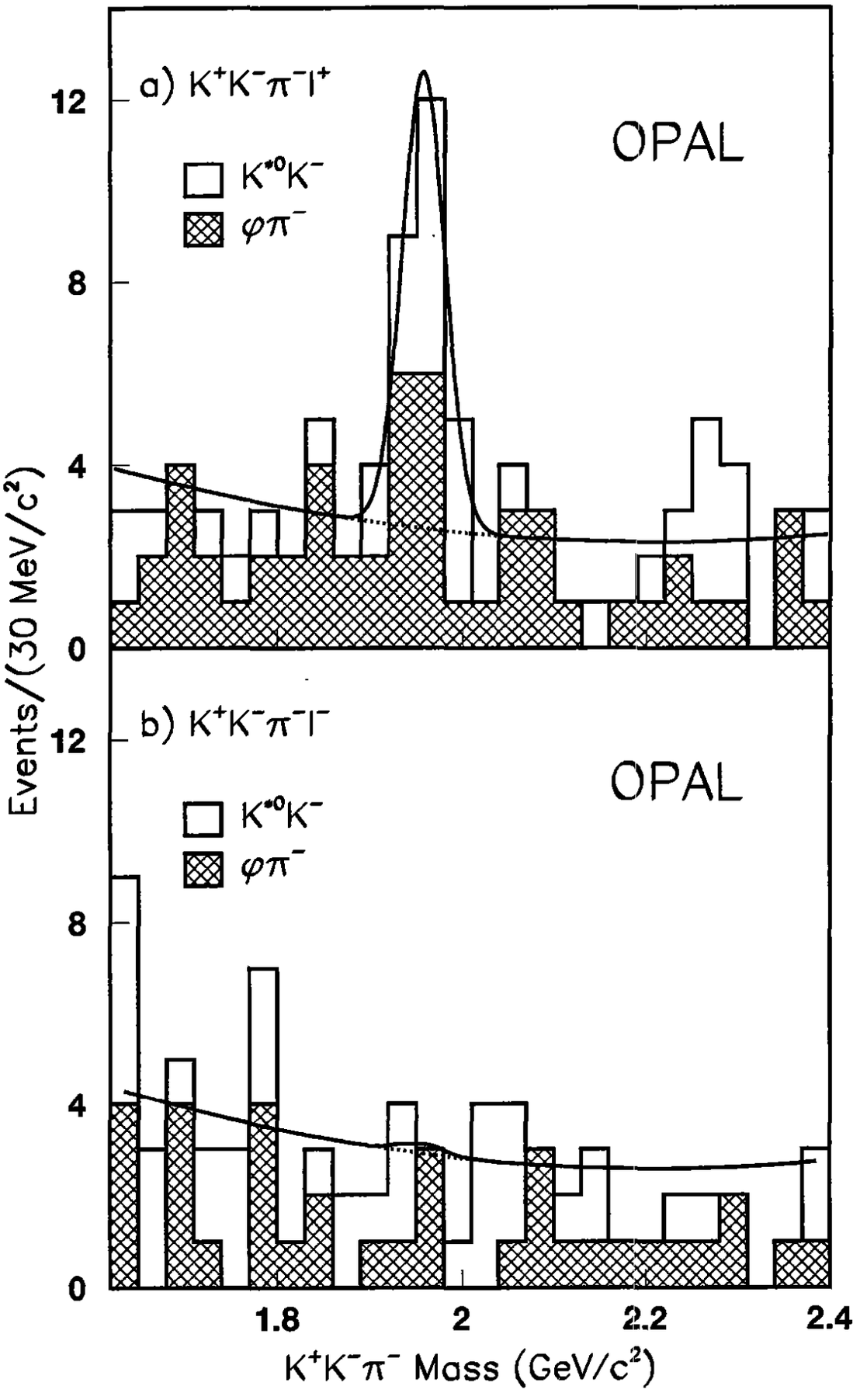
a) $K^+K^-\pi^-l^+$
OPAL
$K^{*0}K^-$
$\varphi\pi^-$
b) $K^+K^-\pi^-l^-$
OPAL
$K^{*0}K^-$
$\varphi\pi^-$
Events/(30 MeV/c^2)
0
4
8
12
1.8
2
2.2
2.4
$K^+K^-\pi^-$ Mass (GeV/c^2)

Figure 6

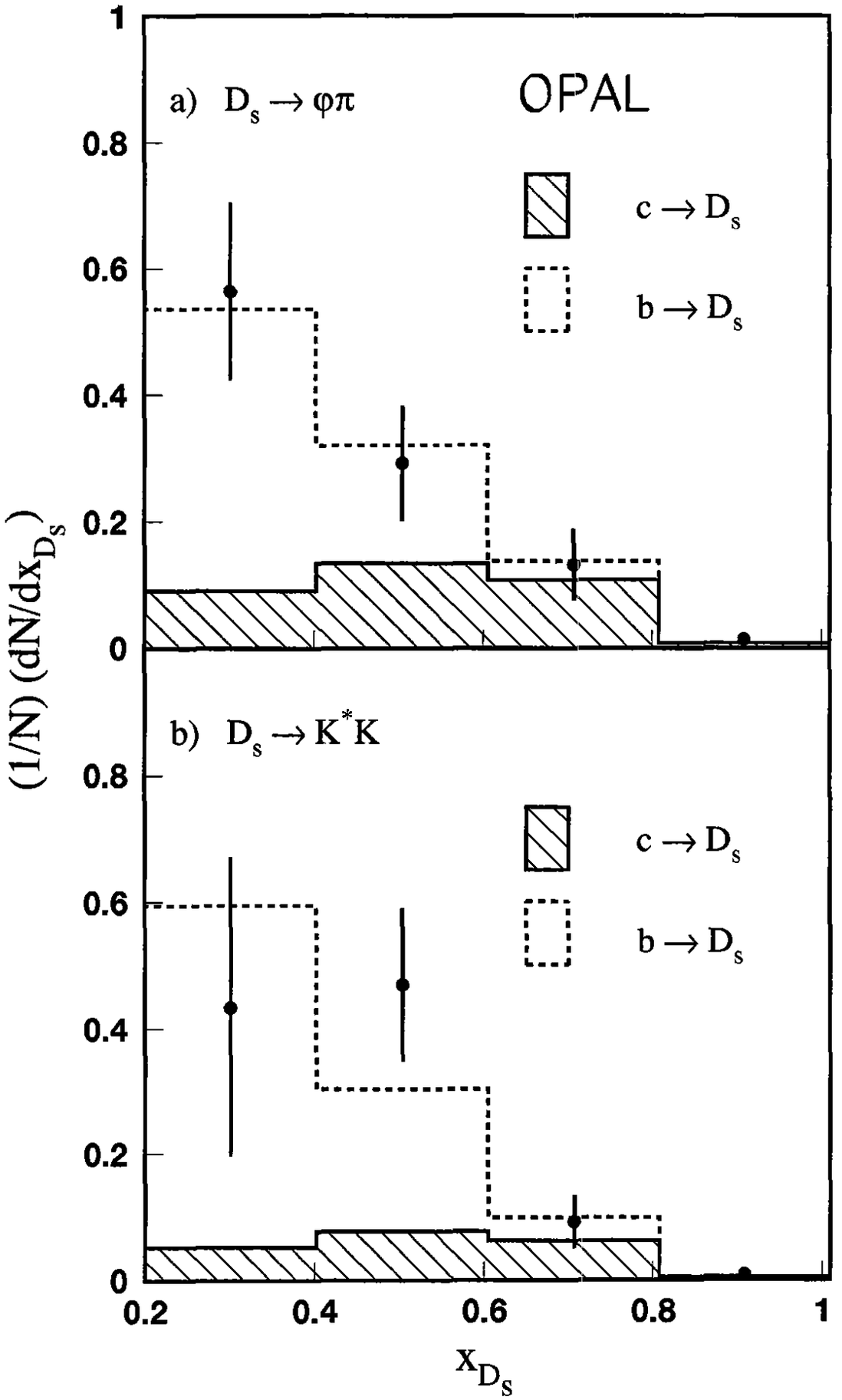
a) $D_s \to \varphi\pi$
OPAL
$c \to D_s$
$b \to D_s$
b) $D_s \to K^*K$
$c \to D_s$
$b \to D_s$
$(1/N)\,(dN/dx_{D_S})$
x_{D_S}
0
0.2
0.4
0.6
0.8
1